Bol. Soc. Paran. Mat.
©SPM – E-ISSN-2175-1188
SPM: www.spm.uem.br/bspm

(3s.) **v. 2025 (43)** : 1–14.
ISSN-0037-8712
doi:10.5269/bspm.77709

Multistage Parker–Sochacki Method for Fractional ODE and PDE Models: Application to the Brusselator System

Saheed Ojo Akindeinde*, Kareem Akanbi Bello and Adebayo Olusegun Adewumi

ABSTRACT: This study presents a novel extension of the Parker–Sochacki method for the numerical solution of the fractional-order Brusselator model, formulated in both ordinary differential equation (ODE) and partial differential equation (PDE) settings. The Brusselator is a canonical model for oscillatory behavior in chemical and biological systems, and its fractional formulation captures memory effects in such dynamics. For the PDE case, the method is combined with the method of lines for efficient treatment of spatially extended systems. A multistage implementation is developed using the Caputo fractional derivative, with an a priori step-size selection based on convergence analysis to ensure stability and accuracy. Numerical simulations confirm the method's effectiveness across different fractional orders. Comparisons with benchmark results demonstrate its accuracy and computational efficiency. The results highlight the influence of the fractional order and show the method's potential for nonlinear fractional differential equations in epidemiology, chemical kinetics, and related fields.

Key Words: Fractional differential equations, Brusselator model, Parker–Sochacki method, Caputo derivative, numerical simulation, pattern formation, multistage methods, reaction–diffusion systems

Contents

1 Introduction **1**

2 Mathematical Preliminaries **2**
2.1 Caputo Fractional Derivative 2
2.2 Fractional-Order Brusselator Model 3

3 The Multistage Parker–Sochacki Method **3**
3.1 Overview of the Classical Parker–Sochacki Method 3
3.2 Extension to Fractional Differential Equations 4
3.3 Multistage Implementation and Step-Size Control 4
3.3.1 A Priori Step-Size Selection 5

4 Extended Fractional PDE Model with Diffusion **5**

5 Numerical Experiments and Results **7**
5.1 Fractional ODE Form of the Brusselator 7
5.1.1 Observed Impact of Fractional Order on System Dynamics 8
5.2 Fractional PDE Form of the Brusselator 11
5.2.1 Effect of the Fractional Order on Spatiotemporal Dynamics 12

6 Conclusion **13**

1. Introduction

Fractional differential equations (FDEs) have become important in modeling complex systems where memory and hereditary effects play a crucial role. Their ability to generalize classical integer-order models makes them suitable for capturing the nonlocal and history-dependent dynamics observed in diverse applications, such as epidemiology, chemical kinetics and control theory [5,9,10,11]. A notable example of such systems is the Brusselator model, a classical reaction–diffusion framework used to study oscillatory behavior and pattern formation in autocatalytic chemical reactions [8,13]. When extended to

* Corresponding author.
2010 *Mathematics Subject Classification:* 34A08, 65L05, 65M06, 35R11, 35K57, 92C45.
Submitted July 07, 2025. Published September 25, 2025

the fractional-order setting, the model becomes capable of describing more intricate dynamics governed by memory effects, making it relevant for modeling infectious disease, spatiotemporal patterning in biology, and other time-sensitive processes.

Despite the theoretical richness of fractional-order formulations, solving the associated equations, especially when extended to partial differential equations (PDEs), remains computationally difficult. Numerous numerical approaches have been proposed to tackle the fractional Brusselator model, such as fractional collocation methods [1], fractal–fractional techniques [2], iterative solvers [3], and wavelet-based schemes [4]. These methods are valuable but often face limitations related to convergence control, computational cost, or generalizability to spatially extended systems.

In the broader context of reaction–diffusion systems, a range of numerical techniques has been developed to address the nonlinear dynamics of the Brusselator model. These include spline-based differential quadrature methods [18], finite difference schemes [19], boundary element formulations [20], and homotopy perturbation methods [21]. There has been limited exploration of extending the application of the Parker–Sochacki method to fractional ordinary differential equations (ODEs), as well as coupling it with the method of lines for solving fractional fractional differential equations (PDEs) using a priori step-size control strategies that ensure convergence and stability in high-order numerical simulations. In our previous work, we contributed to the development of fractional models for infectious disease dynamics [5] and introduced efficient solvers for nonlinear ODEs based on the Parker–Sochacki method [6,7,14,15]. We also proposed a multistage implementation of the method in [15], which improved convergence and computational efficiency in solving nonlinear boundary value problems, including Troesch's equation.

In this study, we build on that foundation and present a novel extension of the Parker–Sochacki method to the fractional Brusselator model in both its ODE and PDE forms. A key innovation of our approach lies in its combination with the method of lines, enabling us to handle the spatial discretization of the PDE version while maintaining the efficiency of the time-domain solver. To ensure numerical stability and convergence, we implement a multistage framework with a priori step-size selection based on theoretical convergence bounds. This eliminates the need for trial-and-error or adaptive step-size control, which are common in existing methods.

The earlier implementations of the Parker–Sochacki method have often relied on symbolic computing platforms, our MATLAB-based implementation demonstrates that the method can be effectively adapted for high-precision numerical simulation of large-scale fractional systems. Numerical simulations demonstrate the impact of the fractional order on the temporal and spatiotemporal behavior of the Brusselator model. The results confirm the method's robustness and flexibility, and comparisons with benchmark solutions in the literature highlight its competitiveness in terms of accuracy and computational efficiency.

The paper is organized as follows. Section 2 presents the relevant preliminaries on fractional calculus. Section 3 describes the multistage Parker–Sochacki method and its convergence analysis. In Section 4, the method is applied to both the ODE and PDE fractional Brusselator models. Section 5 presents the numerical approximations and results. Finally, Section 6 outlines the conclusion.

2. Mathematical Preliminaries

This section outlines the key mathematical tools and formulations that underpin the analysis of the fractional Brusselator model. We begin with a brief overview of the Caputo fractional derivative, which serves as the foundation for the fractional dynamics considered in this study. We introduce the time-fractional and reaction–diffusion forms of the Brusselator model that will be solved numerically in subsequent sections.

2.1. Caputo Fractional Derivative

Among the various definitions of fractional derivatives, the *Caputo derivative* is widely preferred for modeling physical and biological systems due to its natural alignment with classical initial conditions [16]. For a sufficiently smooth function $f \in C^n[0,T]$, the Caputo fractional derivative of order $\alpha \in (n-1,n)$, with $n \in \mathbb{N}$, is defined as

$$ {}^{C}D_t^{\alpha} f(t) = \frac{1}{\Gamma(n-\alpha)} \int_0^t \frac{f^{(n)}(\tau)}{(t-\tau)^{\alpha-n+1}}\, d\tau, \quad t > 0. $$

In the special case $\alpha \in (0,1)$, which is the focus of this work, the definition reduces to

$$ {}^{C}D_t^{\alpha} f(t) = \frac{1}{\Gamma(1-\alpha)} \int_0^t \frac{f'(\tau)}{(t-\tau)^{\alpha}}\, d\tau. $$

A key advantage of the Caputo derivative is that it allows for initial conditions expressed in the classical (integer-order) form $f(0) = f_0$, thereby facilitating the modeling of real-world processes where initial states are physically observable.

2.2. Fractional-Order Brusselator Model

The Brusselator model, introduced in [17], is a prototypical reaction–diffusion system used to model autocatalytic chemical reactions and nonlinear oscillatory dynamics. In this work, we consider its fractional-order formulation to account for memory effects and anomalous transport phenomena.

The time-fractional ordinary differential equation form of the model is given by

$$ \begin{aligned} {}^{C}D_t^{\alpha} x(t) &= B - (A+1)x(t) + x^2(t)y(t), \\ {}^{C}D_t^{\alpha} y(t) &= Ax(t) - x^2(t)y(t), \end{aligned} \tag{2.1} $$

where $\alpha \in (0,1]$ is the fractional order, A and B are positive reaction parameters, and $x(t)$, $y(t)$ denote the concentrations of interacting chemical species over time.

To incorporate spatial diffusion, we consider the reaction–diffusion extension of the model defined over a one-dimensional spatial domain $z \in [0, L]$. The corresponding time-fractional PDE system takes the form:

$$ \begin{aligned} {}^{C}D_t^{\alpha} x(z,t) &= k_1 \frac{\partial^2 x}{\partial z^2} + B - (A+1)x(z,t) + x^2(z,t)y(z,t), \\ {}^{C}D_t^{\alpha} y(z,t) &= k_2 \frac{\partial^2 y}{\partial z^2} + Ax(z,t) - x^2(z,t)y(z,t), \end{aligned} \tag{2.2} $$

where $k_1, k_2 > 0$ are constant diffusion coefficients for the respective species. The system is supplemented with the initial conditions

$$ x(z,0) = x_0(z), \quad y(z,0) = y_0(z), \quad 0 \le z \le L, $$

and boundary conditions of the form

$$ x(0,t) = x(L,t) = B_x(t), \quad y(0,t) = y(L,t) = B_y(t), \quad 0 \le t \le T. $$

This fractional reaction–diffusion system captures both local reaction dynamics and global diffusion-driven interactions, making it suitable for investigating spatiotemporal pattern formation and memory-dependent instabilities. In the next section, we provide a detailed formulation of the multistage Parker – Sochacki method adapted to fractional systems using the Caputo derivative and demonstrate its convergence properties.

3. The Multistage Parker–Sochacki Method

This section presents the implementation of the multistage Parker–Sochacki (PS) method adapted to fractional-order systems involving the Caputo derivative. This was originally developed for classical initial value problems (IVPs), the PS method constructs an explicit power series solution via recursive Picard iteration. Here, we extend the method to handle fractional dynamics and enhance its robustness through a convergence-guided, a priori step-size control mechanism.

3.1. Overview of the Classical Parker–Sochacki Method

The Parker–Sochacki method transforms a system of ordinary differential equations into a polynomial form, enabling the construction of a Maclaurin series solution through a sequence of Picard iterations. Consider the classical IVP:

$$ \frac{dy}{dt} = f(t,y), \quad y(t_0) = y_0. \tag{3.1} $$

The method assumes that $f(t, y)$ can be expressed or approximated as a polynomial, i.e., $f(t, y) = g(y)$, via a process known as polynomial projection [12]. This projection step eliminates the impracticality of iterative symbolic integration and renders the system more amenable to recursive computation.

Applying Picard iteration yields the recurrence:

$$y_{n+1}(t) = y_0 + \int_{t_0}^{t} g(y_n(\tau))\, d\tau, \tag{3.2}$$

which produces a Maclaurin series expansion of the solution:

$$y(t) = \sum_{k=0}^{\infty} y_k (t - t_0)^k, \quad y_0 = a_0. \tag{3.3}$$

Since $g(y)$ is a polynomial, it admits a series representation $g(y) = \sum_{k=0}^{\infty} g_k (t - t_0)^k$. Substituting this into (3.1) yields the recurrence relation for the series coefficients:

$$y_{k+1} = \frac{g_k}{k+1}, \quad k = 0, 1, 2, \ldots \tag{3.4}$$

3.2. Extension to Fractional Differential Equations

To extend the method to fractional-order systems governed by the Caputo derivative, we consider an initial value problem of the form:

$${}^{C}D_t^{\alpha} y(t) = g(y), \quad y(t_0) = y_0, \quad 0 < \alpha \leq 1, \tag{3.5}$$

where $g(y)$ is a polynomial, or can be approximated via polynomial projection. The solution is expressed as a fractional power series:

$$y(t) = \sum_{k=0}^{N} y_k (t - t_0)^{\alpha k}. \tag{3.6}$$

Differentiating term-wise using the Caputo derivative and applying standard identities, we obtain:

$${}^{C}D_t^{\alpha} y(t) = \sum_{k=0}^{N} \frac{\Gamma(\alpha k + \alpha + 1)}{\Gamma(\alpha k + 1)} y_{k+1} (t - t_0)^{\alpha k}. \tag{3.7}$$

In equation (3.5), the right-hand side, $g(y(t))$ is expanded as a fractional power series using the Cauchy product when necessary. Matching both sides of (3.5) term by term leads to the recurrence:

$$y_{k+1} = \frac{\Gamma(\alpha k + 1)}{\Gamma(\alpha k + 1 - \alpha)} g_k, \quad k = 0, 1, 2, \ldots \tag{3.8}$$

The convergence of the series solution of equation (3.6), including its nonlinear Cauchy products, has been rigorously established in [25].

3.3. Multistage Implementation and Step-Size Control

To enhance accuracy and maintain convergence over extended time intervals, we employ a multistage implementation of the PS method. The interval $[0, T]$ is partitioned into M subintervals of uniform step-size $h = T/M$, and the PS method is applied successively within each subinterval. The procedure is as follows:

1. At each subinterval, a truncated fractional power series is computed using the current initial value as the base point.

2. A convergence criterion, derived from bounds on the nonlinear terms, is used to determine an optimal a priori step size h that guarantees convergence of the series within the interval.

3. The terminal value of the series in the current subinterval is used as the initial condition for the next stage.

This approach eliminates the need for adaptive time-stepping or post hoc error correction and ensures that the solution remains within the radius of convergence throughout the simulation. In the next sections, we demonstrate the application of this multistage method to both the ODE and PDE forms of the fractional Brusselator model.

3.3.1. A Priori Step-Size Selection. An essential feature of the multistage Parker–Sochacki method is the ability to select the integration step size based on a theoretical bound that guarantees convergence of the truncated power series. This approach eliminates the need for empirical tuning or adaptive schemes by estimating an optimal step size before each stage of integration.

Theorem 3.1 *Let* $\|\mathbf{y}\| = \max_{1\le i\le n} |y_i|$ *denote the supremum norm for a vector* $\mathbf{y} = (y_1, y_2, \ldots, y_n) \in \mathbb{R}^n$. *Consider a polynomial vector function* $p : \mathbb{R}^d \to \mathbb{R}^d$ *with each component expressible as*

$$p_i(\mathbf{y}) = \sum_{|\alpha|\le k} a_{\alpha,i} Y^\alpha, \quad Y^\alpha = y_1^{\alpha_1} y_2^{\alpha_2} \cdots y_d^{\alpha_d}, \tag{3.9}$$

where $\alpha = (\alpha_1, \ldots, \alpha_d)$ *is a multi-index,* $|\alpha| = \sum_{i=1}^d \alpha_i$, *and* $k = \deg(p_i)$ *is the polynomial degree. Define the quantities*

$$\Sigma p_i = \sum_{|\alpha|\le k} |a_{\alpha,i}|, \quad \Sigma p = \max_i \Sigma p_i, \quad \deg(p) = \max_i \deg(p_i).$$

Let $\mathbf{y}(x)$ *be the solution of the initial value problem*

$$\mathbf{y}' = p(\mathbf{y}), \quad \mathbf{y}(0) = \mathbf{y}_0, \tag{3.10}$$

with $k = \deg(p) \ge 2$. *Set* $\alpha = \max\{1, \|\mathbf{y}_0\|\}$ *and define*

$$M = (k-1)\Sigma p\, \alpha^{k-1}.$$

Then for $|x| < 1/M$, *the truncated Maclaurin series of degree* m *satisfies the error bound*

$$\left\| \mathbf{y}(x) - \sum_{i=0}^{m} \mathbf{y}_i x^i \right\| \le \alpha \frac{(|Mx|)^{m+1}}{1 - |Mx|}.$$

Proof: The detailed proof can be found in [22,23]. □

Based on Theorem 3.1, we estimate the convergence radius of the Maclaurin series as $R = 1/M$. To ensure that the solution remains within this radius, the step size h is selected using a conservative scaling factor:

$$h = \eta R, \quad \text{with } \eta \in (0, 1),$$

where η serves as a safety margin to maintain numerical stability. The apriori step-size strategy is particularly advantageous for stiff or highly nonlinear systems, as it avoids the unpredictability and overhead of dynamic adaptivity. Moreover, it generalizes seamlessly to both ODE and PDE formulations, including systems with spatial diffusion discretized via the method of lines.

4. Extended Fractional PDE Model with Diffusion

To account for spatial heterogeneity and diffusion-driven instability in autocatalytic systems, we extend the classical Brusselator model to a time-fractional reaction–diffusion framework. The model incorporates Caputo fractional derivatives to capture nonlocal temporal dynamics, coupled with standard diffusion terms to represent spatial transport:

$${}^C D_t^\alpha x(z,t) = k_1 \frac{\partial^2 x}{\partial z^2} + B - (A+1)x + x^2 y, \tag{4.1}$$

$${}^C D_t^\alpha y(z,t) = k_2 \frac{\partial^2 y}{\partial z^2} + Ax - x^2 y, \tag{4.2}$$

where $x(z,t)$ and $y(z,t)$ denote species concentrations, $\alpha \in (0,1]$ is the fractional order, and $k_1, k_2 > 0$ are diffusion coefficients. The system evolves over a spatial domain $z \in [0,L]$ and time interval $t \in [0,T]$, with initial conditions

$$x(z,0) = x_0(z), \quad y(z,0) = y_0(z), \quad 0 \le z \le L,$$

and Dirichlet boundary conditions imposed as

$$x(0,t) = x_l(t), \quad x(L,t) = x_r(t), \quad y(0,t) = y_l(t), \quad y(L,t) = y_r(t), \quad 0 \le t \le T.$$

To discretize the system in space, we adopt the method of lines (MOL), dividing the spatial domain into M uniformly spaced nodes $\{z_i\}_{i=1}^{M}$, with spacing $\Delta z = L/(M-1)$. At each interior node $i = 2, \ldots, M-1$, the second-order spatial derivatives are approximated using central finite differences:

$$\frac{\partial^2 x}{\partial z^2} \approx \frac{x_{i-1}(t) - 2x_i(t) + x_{i+1}(t)}{\Delta z^2}, \tag{4.3}$$

$$\frac{\partial^2 y}{\partial z^2} \approx \frac{y_{i-1}(t) - 2y_i(t) + y_{i+1}(t)}{\Delta z^2}. \tag{4.4}$$

To maintain numerical accuracy near boundaries, one-sided approximations are applied at $i = 2$ and $i = M-1$. The boundary values are imposed explicitly:

$$x_1(t) = x_l(t), \quad x_M(t) = x_r(t), \quad y_1(t) = y_l(t), \quad y_M(t) = y_r(t).$$

The spatial discretization transforms the system of PDE into a coupled set of $2(M-2)$ fractional-order ODEs (FODEs) in time:

$${}^{C}D_t^{\alpha} x_i(t) = k_1 \frac{x_{i-1} - 2x_i + x_{i+1}}{\Delta z^2} + B - (A+1)x_i + x_i^2 y_i, \tag{4.5}$$

$${}^{C}D_t^{\alpha} y_i(t) = k_2 \frac{y_{i-1} - 2y_i + y_{i+1}}{\Delta z^2} + A x_i - x_i^2 y_i, \tag{4.6}$$

for $i = 2, \ldots, M-1$.

To evolve the solution in time, we apply the multistage Parker–Sochacki method. Within each subinterval $[t_j, t_{j+1}]$, the solution at each spatial node is approximated via truncated fractional power series:

$$x_i(t) = \sum_{k=0}^{N} a_k^i (t - t_j)^{\alpha k}, \tag{4.7}$$

$$y_i(t) = \sum_{k=0}^{N} b_k^i (t - t_j)^{\alpha k}. \tag{4.8}$$

These expansions are substituted into equations (4.5)–(4.6), and coefficients are matched term-by-term to derive recurrence relations for the series coefficients. For $k \ge 1$, the updates take the form:

$$a_k^i = \frac{\Gamma(\alpha(k-1)+1)}{\Gamma(1+\alpha k)k} \left[k_1 \frac{a_{k-1}^{i-1} - 2a_{k-1}^i + a_{k-1}^{i+1}}{\Delta z^2} + B\delta_{k-1,0} - (A+1)a_{k-1}^i + \sum_{m=0}^{k-1} \sum_{l=0}^{m} a_l^i a_{m-l}^i b_{k-1-m}^i \right], \tag{4.9}$$

$$b_k^i = \frac{\Gamma(\alpha(k-1)+1)}{\Gamma(1+\alpha k)k} \left[k_2 \frac{b_{k-1}^{i-1} - 2b_{k-1}^i + b_{k-1}^{i+1}}{\Delta z^2} + A a_{k-1}^i - \sum_{m=0}^{k-1} \sum_{l=0}^{m} a_l^i a_{m-l}^i b_{k-1-m}^i \right], \tag{4.10}$$

where $\delta_{k,0}$ denotes the Kronecker delta.

The initial coefficients a_0^i and b_0^i are set using the solution values at the start of the subinterval:

$$a_0^i = x_i(t_j), \quad b_0^i = y_i(t_j).$$

Boundary values are enforced at all steps by constraining the coefficients at $i = 1$ and $i = M$:

$$a_k^1 = x_l(t_j)\delta_{k,0}, \quad a_k^M = x_r(t_j)\delta_{k,0}, \quad b_k^1 = y_l(t_j)\delta_{k,0}, \quad b_k^M = y_r(t_j)\delta_{k,0}.$$

This formulation establishes a compact and efficient numerical framework for simulating time-fractional reaction–diffusion systems. By integrating the method of lines with the multistage Parker–Sochacki scheme, we capture both the spatial complexity and temporal nonlocality inherent in fractional chemical dynamics. A structured summary of this implementation is provided in Algorithm 1.

Algorithm 1 Multistage PSM for Fractional PDE Brusselator System

procedure SOLVEBRUSSELATOR($\alpha, A, B, D_x, D_y, L, T_{max}, M, N, h$)
  Initialize spatial grid $z \leftarrow \text{linspace}(0, L, M)$
  Set initial conditions: $x \leftarrow x_0$, $y \leftarrow y_0$
  Enforce Dirichlet BCs at $z = 0, L$
  for $t = h$ to T_{max} step h **do**
    for each interior point z_i **do**
      Compute $\nabla^2 x$, $\nabla^2 y$ via central differences
      Initialize power series: $a_0 \leftarrow x_i$, $b_0 \leftarrow y_i$
      for $k = 1$ to N **do**
        $x2y \leftarrow \sum_{m=0}^{k-1} \sum_{l=0}^{m} a_l a_{m-l} b_{k-1-m}$
        $a_k \leftarrow \frac{\Gamma(\alpha(k-1)+1)}{k\Gamma(\alpha k+1)}[D_x \nabla^2 a_{k-1} + B\delta_{k1} - (A+1)a_{k-1} + x2y]$
        $b_k \leftarrow \frac{\Gamma(\alpha(k-1)+1)}{k\Gamma(\alpha k+1)}[D_y \nabla^2 b_{k-1} + A a_{k-1} - x2y]$
      end for
      Update solutions: $x_i \leftarrow \sum_{n=0}^{N} a_n h^n$, $y_i \leftarrow \sum_{n=0}^{N} b_n h^n$
    end for
    Enforce BCs at current time step
  end for
  return $x(z,t)$, $y(z,t)$
end procedure

5. Numerical Experiments and Results

This section presents comprehensive numerical experiments designed to validate the accuracy and efficiency of the proposed multistage Parker–Sochacki method applied to the fractional-order Brusselator model. Both the fractional ODE and PDE formulations are examined, utilizing the Caputo fractional derivative to capture the system's intrinsic memory effects.

5.1. Fractional ODE Form of the Brusselator

We begin with the time-fractional Brusselator model governed by the Caputo fractional differential system:

$$^C D_t^\alpha x(t) = B - (A+1)x(t) + x^2(t)y(t), \tag{5.1}$$

$$^C D_t^\alpha y(t) = Ax(t) - x^2(t)y(t), \tag{5.2}$$

subject to initial conditions $x(0) = x_0$, $y(0) = y_0$, with fractional order $0 < \alpha \leq 1$.

Invoking Theorem 3.1, the power series solution converges on an interval $(-h, h)$, where the step size h is determined by $h = 1/M$ and

$$\alpha = \max\{1, |x_0|, |y_0|\}, \quad M = 2\alpha^2 \cdot \max\{|A+1| + |B| + 1, |A| + 1\}.$$

For fixed parameters $A = 1.2$, $B = 0.5$, and initial values $x_0 = y_0 = 1$, we compute $M = 3.7$ and select a convergent step size $h = 0.1$ using a safety factor $\eta = 0.8$. The multistage Parker–Sochacki method is then applied over the time interval $[0, 20]$.

Under the condition $1 - A + B^2 \geq 0$, the system is expected to exhibit a stable limit cycle, as confirmed in Figure 1. The time series and phase portraits depict the oscillatory dynamics of $x(t)$ and $y(t)$, while accompanying distance and autocorrelation analyses confirm the limit cycle's stability.

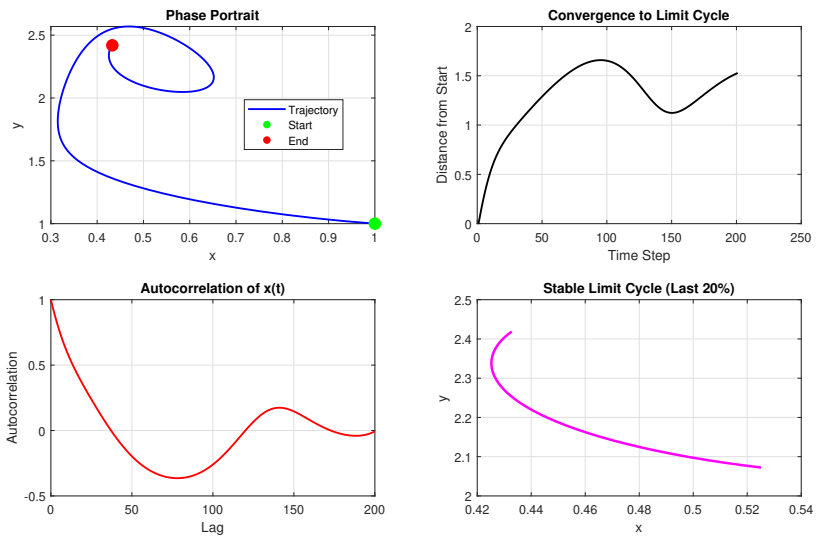

(a) Time evolution of concentrations $x(t)$ and $y(t)$.

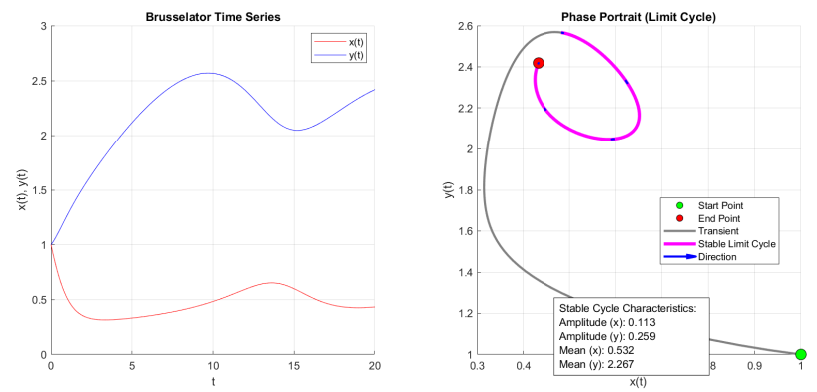

(b) Phase portrait illustrating the stable limit cycle.

Figure 1: Dynamical behavior of the fractional Brusselator model for the classical case $\alpha = 1$.

Further insights into the influence of the fractional order α on system dynamics are provided in Figures 2 and 3. These figures display both the temporal evolution and phase portraits of (x, y) for varying α, demonstrating how decreasing the fractional order attenuates the oscillatory behavior and affects stability characteristics.

5.1.1. Observed Impact of Fractional Order on System Dynamics. Numerical simulations of the fractional Brusselator model, as illustrated in Figures 2 and 3, demonstrate that the values of $x(60)$ and $y(60)$ vary significantly with different choices of the fractional order α. This notable variation at a fixed final time underscores the substantial influence of the fractional order on the system's long-term behavior.

Because the fractional derivative inherently captures memory effects and nonlocal temporal depen-

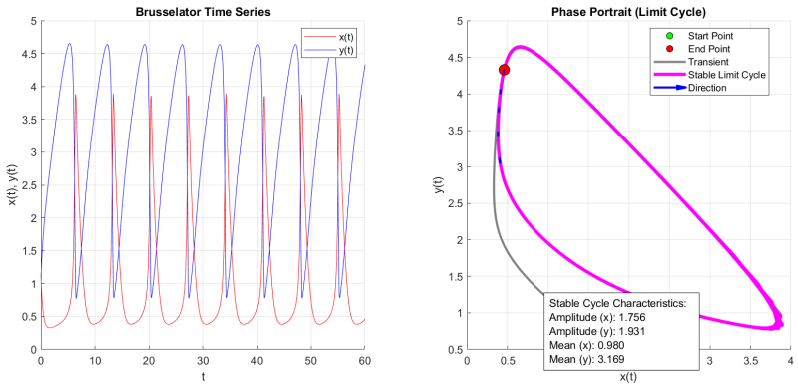

(a) Dynamics for $\alpha = 1$.

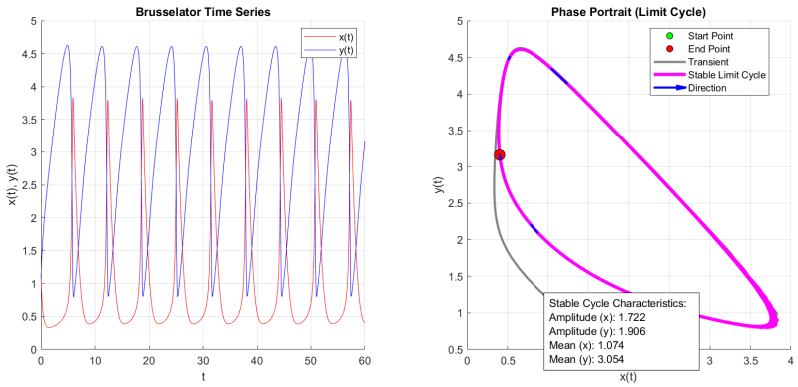

(b) Dynamics for $\alpha = 0.8$.

Figure 2: Time series and phase portraits of the fractional Brusselator system for $A = 3$, $B = 1$ at selected fractional orders.

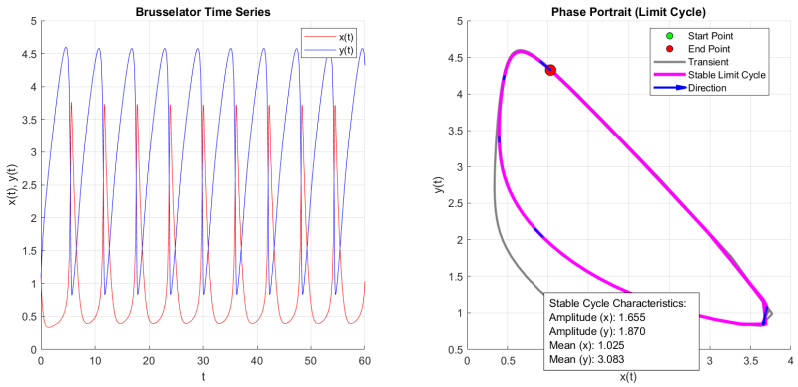

(a) Dynamics for $\alpha = 0.6$.

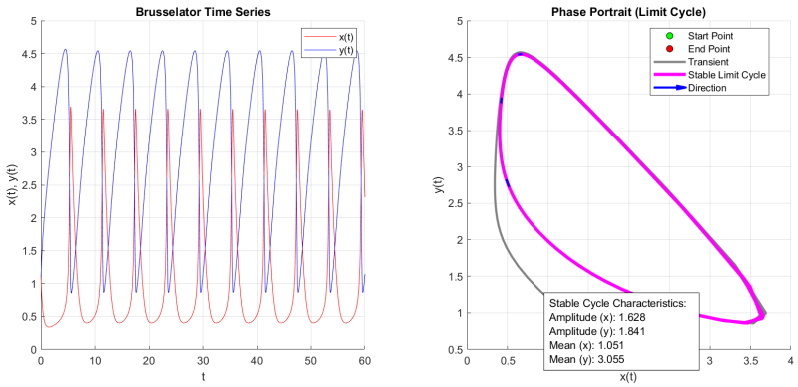

(b) Dynamics for $\alpha = 0.4$.

Figure 3: Time series and phase portraits illustrating the effect of lower fractional orders on the Brusselator dynamics with $A = 3$, $B = 1$.

dencies, adjusting α modifies the system's effective evolution rate. Consequently, the sensitivity of the solution to α highlights the importance of fractional-order modeling in representing richer and more complex reaction dynamics beyond the capabilities of classical integer-order models.

5.2. Fractional PDE Form of the Brusselator

We consider the fractional partial differential equation formulation of the Brusselator model as presented in equations (5.1) and (5.2) subject to the initial conditions

$$x(z,0) = B + z(1-z), \quad y(z,0) = \frac{A}{B} + z^2(1-z),$$

and Dirichlet boundary conditions

$$x(0,t) = x(b,t) = B, \quad y(0,t) = y(b,t) = \frac{A}{B}, \quad 0 \le t \le b.$$

The following parameters are considrered: $A = 0.2, B = 0.6$ and $k_1 = k_2 = \frac{1}{40}$. The spatial domain $z \in [0,1]$ is discretized via finite differences using the method of lines. The resulting system of time-fractional ordinary differential equations is integrated in time employing the multistage Parker-Sochacki method described in Section 4.

The simulation results shown in Figure 4 replicate those obtained in [24] using a time-splitting approach under identical parameter settings, thereby validating our approach. Additional simulations with parameters $A = 3$ and $B = 1$ are presented in Figures 5a–5d, illustrating the formation of complex spatial patterns and temporal oscillations that evolve as the fractional order α varies.

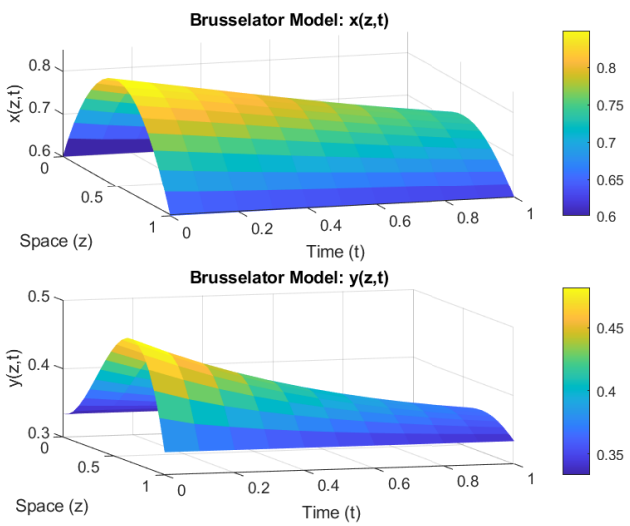

Figure 4: Spatiotemporal evolution of chemical concentrations for the fractional PDE Brusselator model with $\alpha = 1$.

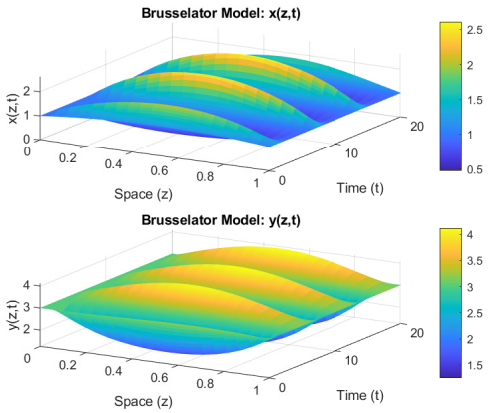

(a) Time series and phase portrait for $\alpha = 1$.

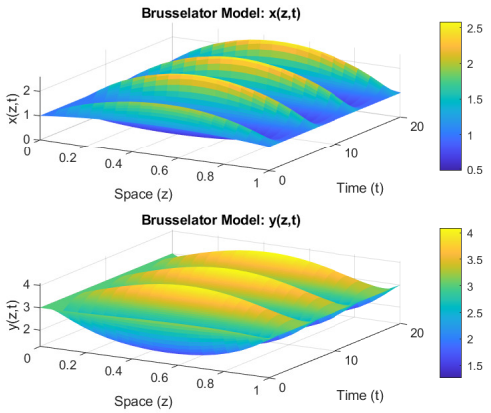

(b) Spatiotemporal pattern for $\alpha = 0.8$.

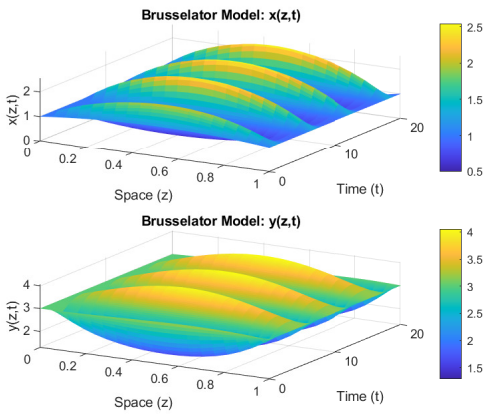

(c) Spatiotemporal pattern for $\alpha = 0.6$.

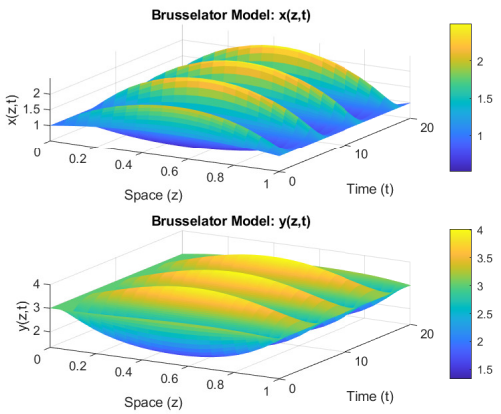

(d) Spatiotemporal pattern for $\alpha = 0.4$.

Figure 5: Spatiotemporal dynamics of the fractional Brusselator model with Dirichlet boundary conditions, demonstrating the effect of varying fractional order α.

5.2.1. Effect of the Fractional Order on Spatiotemporal Dynamics. Figure 5 illustrates the profound influence of the fractional order α on the spatiotemporal dynamics of the Brusselator model under Dirichlet boundary conditions. In the classical limit $\alpha = 1$, the system sustains periodic oscillations with well-defined spatially periodic structures, indicative of robust reaction–diffusion coupling.

As α decreases from unity, memory effects inherent in the Caputo fractional derivative begin to dominate the system's temporal behavior. For $\alpha = 0.8$, the spatiotemporal patterns persist but exhibit mild damping, suggesting a slower temporal response. At $\alpha = 0.6$, the oscillations become significantly attenuated, and the spatial coherence diminishes, indicating that the system is transitioning away from a sustained oscillatory regime.

By the time α is reduced to 0.4, the dynamics are heavily suppressed: oscillatory behavior is lost, and spatial organization becomes increasingly diffuse. The system settles into a subdued dynamical regime, characterized by slow diffusion-dominated relaxation.

These observations highlight the critical role of the fractional order in modulating the persistence and structure of chemical oscillations and patterns. Lower values of α introduce stronger memory and nonlocal temporal effects, which act to dampen the system's reactivity and spatial complexity, ultimately controlling the emergence and sustainability of spatiotemporal structures.

6. Conclusion

The study has developed and demonstrated a multistage implementation of the Parker–Sochacki method tailored for fractional-order systems involving the Caputo derivative. By reformulating the classical Parker–Sochacki power series approach to accommodate fractional derivatives, and integrating it with a convergence-driven step-size control strategy, we have established an accurate and computationally efficient framework for solving both fractional ordinary and partial differential equations.

The effectiveness of the method was validated through extensive numerical experiments on the fractional Brusselator model. In the case of ODE, the method successfully captured the system's oscillatory dynamics and the influence of the fractional order on long-term behavior. In the PDE setting, spatial discretization via the method of lines combined with multistage power series integration enabled the simulation of complex spatiotemporal patterns.

The results reveal that the fractional order of the α values significantly affects the qualitative behavior of the system. In particular, lower values of α, representing stronger memory effects, led to damping of oscillations and loss of spatial coherence, both in temporal trajectories and in reaction–diffusion patterns. These findings emphasize the importance of fractional modeling in capturing rich dynamics not observable in classical integer-order formulations.

Beyond the Brusselator model, the proposed multistage Parker–Sochacki method offers a general-purpose tool for fractional dynamical systems, with potential applications in physics, biology, and engineering domains where memory and nonlocal effects are essential. Future work may explore its extension to higher-dimensional spatial domains, systems with variable-order derivatives, and coupling with stochastic components.

References

1. Izadi, M., and Srivastava, H. M., *Fractional clique collocation technique for numerical simulations of fractional-order Brusselator chemical model*, Axioms, 11(11), 654, (2022).
2. Saad, K. M., *Fractal-fractional Brusselator chemical reaction*, Chaos, Solitons & Fractals, 150, 111087, (2021).
3. Asv, R. K., and Devi, S., *A novel three-step iterative approach for oscillatory chemical reactions of fractional Brusselator model*, International Journal of Modelling and Simulation, 43(5), 559–578, (2023).
4. Manohara, G., and Kumbinarasaiah, S., *Fibonacci wavelet collocation method for the numerical approximation of fractional order Brusselator chemical model*, Journal of Mathematical Chemistry, 62(10), 2651–2681, (2024).
5. Akindeinde, S. O., Okyere, E., Adewumi, A. O., Lebelo, R. S., Fabelurin, O. O., and Moore, S. E., *Caputo fractional-order SEIRP model for COVID-19 Pandemic*, Alexandria Engineering Journal, 61(1), 829–845, (2022).
6. Akindeinde, S. O., and Okyere, E., *New analytic technique for the solution of nth-order nonlinear two-point boundary value problems*, Journal of Advances in Mathematics and Computer Science, 15(2), 1–11, (2016).
7. Akindeinde, S. O., *Improved Parker–Sochacki method for closed form solution of two and three-point boundary value problems of nth-order ODEs*, International Journal of Applied Mathematics, 29(5), 1–11, (2016).
8. Golovin, A. A., Matkowsky, B. J., and Volpert, V. A., *Turing pattern formation in the Brusselator model with superdiffusion*, SIAM Journal on Applied Mathematics, 69(1), 251–272, (2008).
9. Ahmed, I., Baba, I. A., Yusuf, A., Kumam, P., and Kumam, W., *Analysis of Caputo fractional-order model for COVID-19 with lockdown*, Advances in Difference Equations, 2020(1), (2020).
10. Rajagopal, K., Hasanzadeh, N., Parastesh, F., Hamarash, I. I., Jafari, S., and Hussain, I., *A fractional-order model for the novel coronavirus (COVID-19) outbreak*, Nonlinear Dynamics, 101(1), 711–718, (2020).
11. Wang, H., Jahanshahi, H., Wang, M. K., Bekiros, S., Liu, J., and Aly, A. A., *A Caputo-Fabrizio Fractional-Order Model of HIV/AIDS with a Treatment Compartment: Sensitivity Analysis and Optimal Control Strategies*, Entropy, 23(5), 610, (2021).
12. Akindeinde, S. O., *A new multistage technique for approximate analytical solution of nonlinear differential equations*, Heliyon, 6(10), e05266, (2020).
13. Yuan, Q., Wang, S., Lai, T., & Wang, H. *Spatiotemporal fluctuation induces Turing pattern formation in the chemical Brusselator*, Mathematical Methods in the Applied Sciences, 48(3), 3233–3252, (2025).
14. Akindeinde, S. O., *Parker–Sochacki method for the solution of convective straight fins problem with temperature-dependent thermal conductivity*, International Journal of Nonlinear Sciences, 25(2), 119–128, (2018).
15. Akindeinde, S. O., Adesanya, S. O., Lebelo, R. S., and Moloi, K. C., *A new multistage Parker–Sochacki method for solving the Troesch's problem*, International Journal of Engineering & Technology, 9(2), 592–601, (2020).

16. Caputo, M., and Fabrizio, M., *A new definition of fractional derivative without singular kernel*, Progress in Fractional Differentiation & Applications, 1(2), 73–85, (2015).

17. Prigogine, I., and Lefever, R., *Symmetry breaking instabilities in dissipative systems. II*, Journal of Chemical Physics, 48(4), 1665–1700, (1968).

18. Jiwari, R., and Yuan, J., *A modified cubic B-spline differential quadrature method for reaction–diffusion systems*, Applied Mathematics and Computation, 398, 125865, (2022).

19. Twizell, E. H., et al., *A second-order finite-difference method for solving reaction–diffusion equations*, Journal of Computational and Applied Mathematics, 63(2), 259–270, (1995).

20. Ang, W. H., *Application of the dual-reciprocity boundary element method to nonlinear reaction–diffusion systems*, Engineering Analysis with Boundary Elements, 28(12), 1455–1463, (2004).

21. Khan, Y. & Wu, Q. *Homotopy perturbation method for solving nonlinear reaction–diffusion systems*, Computers & Mathematics with Applications, 59(10), 3320–3327, (2010).

22. Pouly, A., and Graca, D. S., *Computational complexity of solving polynomial differential equations over unbounded domains*, Theoretical Computer Science, 626, 67–82, (2016).

23. Warne, P. G., Warne, D. A. P., Sochacki, J. S., Parker, G. E., and Carothers, D. C., *Explicit a-priori error bounds and adaptive error control for approximation of nonlinear initial value differential systems*, Computers & Mathematics with Applications, 52(12), 1695–1710, (2006).

24. Uysal, S. Ö. K., and Çiçek, Y., *Numerical solution of the Brusselator model by time splitting method*, Cumhuriyet Science Journal, 42(1), 75–87, (2021).

25. Jornet, M., *Power-series solutions of fractional-order compartmental models*, Comput. Appl. Math., 43, (2024).

Saheed Ojo Akindeinde,
Department of Mathematics and Statistical Sciences,
Botswana International University of Science and Technology,
Botswana.
https://orcid.org/0000-0003-2513-1237
E-mail address: akindeindes@biust.ac.bw

and

Kareem Akanbi Bello,
Department of Mathematics,
University of Ilorin,
Nigeria.
https://orcid.org/0009-0007-6270-7705
E-mail address: bello.ak@unilorin.edu.ng

and

Adebayo Olusegun Adewumi,
Department of Mathematics,
Obafemi Awolowo University,
Nigeria.
https://orcid.org/0000-0002-1335-4567
E-mail address: aoadewumi@oauife.edu.ng